

## Recent studies with fast RI beams of interest in nuclear structure and astrophysics

T. Motobayashi<sup>a</sup>

<sup>a</sup>RIKEN, 2-1 Hirosawa, Wako, Saitama 351-0198, Japan

Nuclear spectroscopy and nuclear astrophysics using fast radio-isotope (RI) beams has been developed. At the RIKEN Accelerator Research Facility, direct-reaction experiments have been performed at incident energies of a few tens MeV/nucleon in the reversed kinematics. Nuclear levels in the final state of the reaction are separated by measuring the invariant mass when the excited state of interest is particle unbound or by measuring deexcitation  $\gamma$  rays for bound excited levels. Several highlights in recent studies are presented.

### 1. INTRODUCTION

Since 1990s radio-isotope (RI) beams have been provided at the RIKEN Accelerator Research Facility. Since the projectile-fragmentation scheme is used, the energy resolution of the separated RI beam is poor (a few %) and the intensity is low so that a thick target is favored. This makes the experiment quite difficult, especially in measuring the missing mass to separate nuclear levels in the final state. We overcome these difficulties by adopting mainly two methods. One is to measure the invariant mass if the excited state of interest is particle unbound. For bound states, deexcitation  $\gamma$  rays are measured to identify the excited levels.

Coulomb excitation has been studied to study bound excited states with beams of unstable nuclei. Comparing the yield of deexcitation  $\gamma$  rays and theoretical prediction of the Coulomb excitation cross section, the transition probability of the relevant state can be extracted. We built an array of NaI(Tl) scintillators called DALI, and measured the probabilities of the  $2^+-0^+$  transitions in  $^{32}\text{Mg}$  [1],  $^{34}\text{Mg}$  [2],  $^{56}\text{Ni}$  [3], etc, and the E1 transitions in  $^{11}\text{Be}$  [4],  $^{12}\text{Be}$  [5] and  $^{15}\text{O}$  [6]. The method of  $\gamma$ -ray detection was extended recently to (p,p') [7] and (d,d') [8] reactions. Efficient measurements were realized by using a liquid hydrogen target. The locations of the first and second excited states in  $^{34}$  have been determined by a new method of  $\gamma$ -ray spectroscopy using projectile fragmentation of secondary beams [9].

One of the recent highlights is measurements for the  $2^+-0^+$  transition in  $^{16}\text{C}$ . A lifetime measurement [10] and a  $^{16}\text{C}+\text{Pb}$  inelastic scattering experiment [11] point to a surprising nature of the transition: very much hindered E2 and enhanced neutron excitation.

In the invariant mass method, particles decaying in flight is measured. The method has been applied to astrophysical (p, $\gamma$ ) processes by measuring the products of Coulomb dissociation. The processes with p-shell nuclei, such as  $^8\text{B}\rightarrow^7\text{Be}+\text{p}$  [12],  $^9\text{C}\rightarrow^8\text{B}+\text{p}$ , and

$^{14}\text{O} \rightarrow ^{13}\text{N} + \text{p}$  [13] have been measured with a lead target. Recently we extended the study to a few rp-process nuclei as  $^{22}\text{Mg} \rightarrow ^{23}\text{Al}$  [14].

Another application of the Coulomb dissociation is to measure the E1 strength function of very neutron-rich nuclei as  $^{11}\text{Li}$  [15] and  $^{19}\text{C}$  [16]. The invariant mass method was applied also to the charge-exchange reactions. The isobaric analog states of  $^{11}\text{Li}$  and  $^{14}\text{Be}$  in  $^{11}\text{Be}$  [17] and  $^{14}\text{B}$  [18], respectively, were excited by the (p,n) reaction in reverse kinematics. Their location was determined by measuring the three-body decay channels of the analog states.

Encouraged by these results, we plan to extend studies to more exotic and heavier nuclei in the RIKEN RI Beam Factory, which is expected to come into operation during the year 2006.

## 2. SPECTROSCOPY OF $^{12}\text{Be}$

Figure 1 shows the level scheme of the neutron rich nucleus with a neutron magic number  $N=8$ . The state at 2.7 MeV is assigned to be  $1^-$  by comparing the  $\gamma$  ray spectra obtained by  $^{12}\text{Be} + ^{208}\text{Pb}$  and  $^{12}\text{Be} + ^{12}\text{C}$  inelastic scattering [5]. The transition is clearly seen for the former case, while it is not observed in the  $^{12}\text{Be} + ^{12}\text{C}$  spectrum. This is a characteristic feature of E1 ( $\ell=1$ ) transitions. An isomeric state at 2.24 MeV was found recently [19]. Its spin  $0^+$  was determined by the  $\gamma$ - $\gamma$  angular correlation for the cascade of  $0_2^+ - 2^+ - 0_1^+$ . The locations of these states are much lower than the ones in neighboring  $N=8$  nuclei, indicating that the neutron shell closure is obliterated in  $^{12}\text{Be}$ .

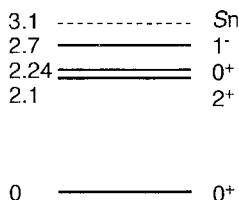


Figure 1. Level diagram of  $^{12}\text{Be}$ . The states at 2.24 MeV and 2.7 MeV have been found by experiments with fast RI beams of  $^{12}\text{Be}$ .

## 3. NUCLEI AROUND $N=20$

Studies of neutron-rich nuclei around  $N=20$  have been performed. The first Coulomb excitation experiment has been made for  $^{32}\text{Mg}$  [1]. Radioactive  $^{32}\text{Mg}$  beams of around 300 cps with an average energy of 49.2 MeV/nucleon bombarded a  $^{208}\text{Pb}$  target with 350 mg/cm<sup>2</sup> thickness, and  $\gamma$  rays from the  $2^+$  state in  $^{32}\text{Mg}$  were detected. The extracted large  $B(\text{E}2)$  value of  $454 \pm 78 \text{ e}^2 \text{ fm}^4$  supports the idea of disappearance of the  $N=20$  shell closure in  $^{32}\text{Mg}$ .

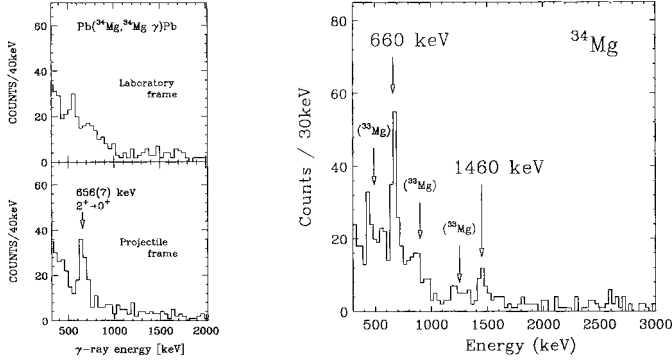


Figure 2. Spectra of  $\gamma$  rays associated with the inelastic  $^{34}\text{Mg} + \text{Pb}$  scattering (left) and the  $^{36}\text{Si} + ^9\text{Be} \rightarrow ^{34}\text{Mg} + \text{X}$  fragmentation (right).

The Coulomb excitation technique was applied to the more neutron rich nucleus  $^{34}\text{Mg}$  with only  $4 \text{ s}^{-1}$  intensity of the beam [2]. The left panel of Fig. 2 shows spectra of  $\gamma$  rays measured in coincidence with outgoing particles identified as  $^{34}\text{Mg}$ . The spectrum in the moving frame (bottom) was obtained by correcting for the Doppler shift arising from the high velocity ( $\beta \approx 0.3$ ) of the  $\gamma$ -emitter. This correction was made by the  $\gamma$ -ray emission angle measured by the NaI(Tl) array DALI, which consisted of 66 crystals with the size of  $6 \times 6 \times 12 \text{ cm}^3$ . As shown in the figure, a clear peak is observed at around 656 keV which corresponds to the  $2^+ - 0^+$  transition in  $^{34}\text{Mg}$ . From the yield of the peak, one can extract the Coulomb excitation cross section and hence the electromagnetic transition probability  $B(E2)$ . The extracted large  $B(E2)$  value around  $600 \text{ e}^2 \text{ fm}^4$  corresponds to the quadrupole deformation  $\beta_2 \approx 0.6$ , which is even larger than  $\approx 0.5$  for  $^{32}\text{Mg}$  [1]. This supports the picture of well-developed deformation suggested by the result of our  $\gamma$ -ray spectroscopy with the two-step fragmentation scheme [9]. A secondary radioactive  $^{36}\text{Si}$  beam produced by  $^{40}\text{Ar}$  fragmentation bombarded a beryllium target, and  $^{34}\text{Mg}$  fragments and their deexcitation  $\gamma$ -rays were detected in coincidence. Compared with  $\gamma$ -ray measurements with  $^{40}\text{Ar}$  fragmentation, a larger cross section of  $^{36}\text{Si} \rightarrow ^{34}\text{Mg}$  allows the use of intense primary beams, because the measurement is almost free from large background due to unwanted products. The two peaks at 660 keV and 1460 keV (Fig 2) may correspond respectively to the  $2^+ - 0^+$  and  $4^+ - 2^+$  transitions in  $^{34}\text{Mg}$ . The ratio of the energies  $E(4^+)/E(2^+)$  is calculated to be 3.2, which is very close to the value 3.3 expected for a rigid rotor, indicating that  $^{34}\text{Mg}$  is a nucleus with well-developed quadrupole deformation.

Another nucleus of interest is  $^{30}\text{Ne}$ , the most proton deficient even-even nucleus with  $N=20$ . To overcome the very weak  $^{30}\text{Ne}$  beam intensity of 0.2 cps, a liquid hydrogen target was employed to observe the  $2^+ - 0^+$   $\gamma$  transition. We have succeeded to determine the location of the first  $2^+$  state to be  $791 \pm 26 \text{ keV}$  [7], which is lower than that of  $^{32}\text{Mg}$ .

Figure 3 summarizes  $B(E2)$  for even-even nuclei with  $N=20$ . As clearly seen, the

values for  $^{32}\text{Mg}$  and  $^{30}\text{Ne}$  are larger than other less proton deficient nuclei, indicating disappearance of the shell closure for the two nuclei.

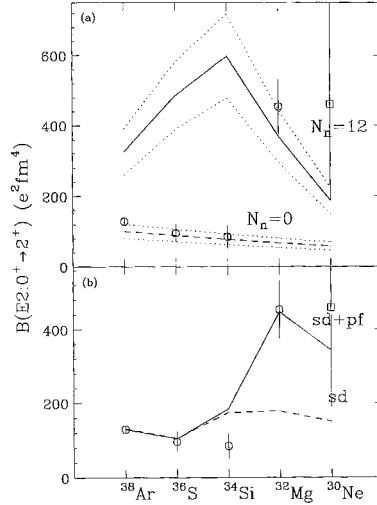


Figure 3. Reduced transition probability  $B(E2)$  of  $N=20$  even-even nuclei. The value for  $^{30}\text{Ne}$  is estimated from the deformation parameter extracted from the  $(p,p')$  cross section assuming that the Coulomb deformation is equal to the matter deformations. The lines represent predictions of (a) the  $N_p N_n$  scheme [20] and (b) the shell model predictions by Fukunishi, Otsuka and Sebe [21].

On the other hand,  $^{34}\text{Si}$  is regarded as spherical from its high  $2^+$  excitation energy and a small  $0^+ \rightarrow 2^+$  transition probability. A candidate of the second  $0^+$  state, which is related to the “shape coexistence” picture for  $^{34}\text{Si}$ , has been suggested 1.193 MeV below the  $2^+$  state by a  $\beta$  decay study [22]. Figure 4 shows the  $\gamma$  ray spectrum measured in coincidence with the  $2^+ \rightarrow 0^+$  transition associated with the  $^{34}\text{Si}(d,d')$  reaction in reversed kinematics. A  $\gamma$  line with 1.193 MeV energy is clearly seen, indicating that this line cannot be the  $2^+ \rightarrow 0_2^+$  transition as is suggested in Ref. [22]. The high  $\gamma$  efficiency of DALI enabled the  $\gamma$ - $\gamma$  coincidence measurement with high statistics.

#### 4. ANOMALY IN $^{16}\text{C}$

Recently, the  $2^+$  state in the neutron-rich nucleus  $^{16}\text{C}$  has been studied by a lifetime measurement and inelastic scattering with a lead target. Its extremely long lifetime of  $75 \pm 23$  ps (corresponding to 0.3 WU) [10] and a large hindrance of the Coulomb excitation amplitude compared with the nuclear excitation amplitude [11] consistently point to a

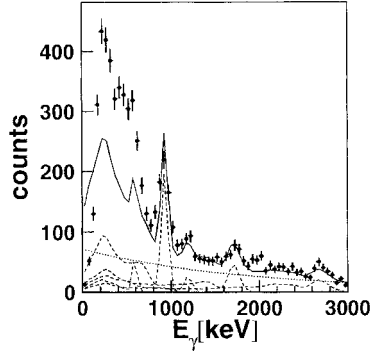


Figure 4. Spectrum of  $\gamma$  rays measured in coincidence with the  $2^+-0^+$  transition in  $^{34}\text{Si}$ .

picture that the  $2^+$  state is excited almost solely by neutron excitation. This suggests decoupling of neutron and proton motions, which is quite unique.

## 5. COULOMB DISSOCIATION STUDIES FOR ASTROPHYSICAL RADIATIVE CAPTURE

Coulomb dissociation is useful in studying radiative capture reactions of astrophysical interest. Its large cross section and high experimental efficiency enable one to study reactions involving unstable nuclei. Coulomb dissociation is regarded as absorption of virtual photons, and hence related to the photo disintegration process, the inverse of the radiative capture of interest [23]. Based on the experimental method developed at RIKEN [13,12], we applied the Coulomb dissociation technic to the reaction  $^{22}\text{Mg}(p,\gamma)^{23}\text{Al}$  [14], which is expected to be involved in the rapid-proton process relevant to nuclear burning in Novae.

RI beams of  $^{23}\text{Al}$  bombarded a Pb target, and fragments of Coulomb dissociation,  $^{22}\text{Mg}$  and a proton, were detected in coincidence. From their energies and emission angles, we extracted the  $p$ - $^{22}\text{Mg}$  relative energy corresponding to the center-of-mass energy of the  $(p,\gamma)$  reaction. Figure 5 shows the relative energy spectrum. A peak at around 400 keV corresponds to the resonance in  $^{23}\text{Al}$  at the excitation energy of 528 keV, which is expected to play a crucial role in nova burning. The extracted radiative width of this state, the spin of which is expected to be  $1/2^+$ , is  $0.72 \pm 0.14 \mu\text{eV}$ . The result is closed to the theoretical estimate by Caggiano *et al.* [24], and thus confirms their conclusion that the reaction plays a role only at very high temperature. To reach the same statistical level, a direct  $(p,\gamma)$  measurement with a low energy RI beam requires intensity of approximately  $10^{12}$  particle per second, indicating that the Coulomb dissociation is the only method to determine the radiative width in practice.

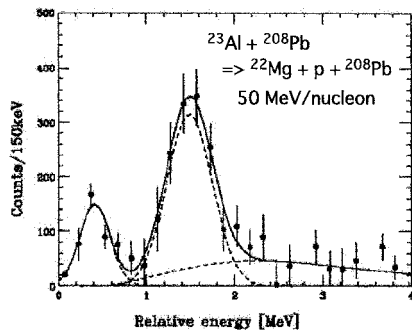


Figure 5. Relative energy spectrum for the Coulomb dissociation reaction  $^{208}\text{Pb}(^{23}\text{Al},p)^{22}\text{Mg}$  measured at  $E_{\text{in}}=50$  MeV/nucleon.

## 6. RIBF PROJECT

Encouraged by achievements of various studies with RI beams, RIKEN has started to build a new RI beam facility called RI Beam Factory (RIBF). A schematic view of the RIKEN accelerator complex is shown in Fig. 6. The existing facility consists of two injectors, an AVF (azimuthally varying field) cyclotron for ions up to Kr and a linac (RILAC) for heavier ions, and a main ring cyclotron (RRC) with  $K=540$  MeV. RI-beams with  $Z < 30$  are mainly produced by RIPS seen in the left of the figure.

In RIBF, heavy ion beams from the RILAC-RRC combination are injected to the new ring cyclotrons, fRC (fixed-energy Ring Cyclotron), IRC (Intermediate-stage Ring Cyclotron) and SRC (Superconducting Ring Cyclotron). Beams with 350 MeV/nucleon energy are available for entire range of atomic mass. The maximum beam intensity is planned to be 1  $\mu\text{A}$ . RI beams are produced by projectile fragmentation and in-flight fission. The energy of produced RI beams is 200–300 MeV/nucleon.

The first RI beam through the SRC and BigRIPS will be in 2006 and first experiments are expected to start in 2007. The first phase of RIBF construction includes all the cyclotrons, BigRIPS and RI-beam transport including (at least) a part of the zero-degree spectrometer which identifies products of secondary reactions. The second phase with extended experimental equipments is under consideration.

## REFERENCES

1. T. Motobayashi *et al.*, Phys. Lett. B346 (1995) 9.
2. H. Iwasaki *et al.*, Phys. Lett. B522 (2001) 227.
3. Y. Yanagisawa *et al.*, Proc. Int. Conf. Exotic Nuclei and Atomic Masses, AIP Conf. Proc. 435 (1998) 610.

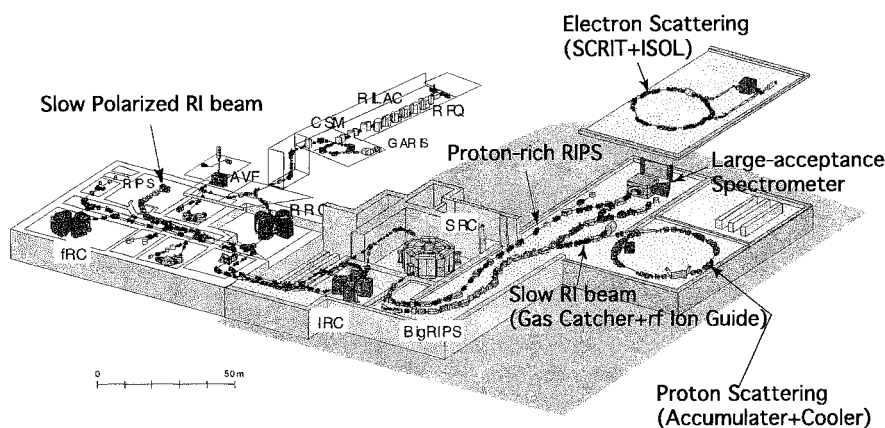


Figure 6. Schematic view of the RIKEN accelerator complex. The shaded areas are for RIBF.

4. T. Nakamura *et al.*, Phys. Lett. B394 (1997) 11.
5. H. Iwasaki *et al.*, Phys. Lett. B491 (2000) 8.
6. K. Yamada *et al.*, Phys. Lett. B579 (2004) 265.
7. Y. Yanagisawa *et al.*, Phys. Lett. B566 (2003) 84.
8. N. Iwasa *et al.*, Phys. Rev. C67 (2003) 064315.
9. K. Yoneda *et al.*, Phys. Lett. B499 (2001) 233.
10. N. Imai *et al.*, Phys. Rev. Lett. in print.
11. Z. Elekes *et al.*, to be published.
12. T. Motobayashi *et al.*, Phys. Rev. Lett. 73 (1994) 2680; N. Iwasa *et al.*, J. Phys. Soc. Jpn. 65 (1996) 1256; T. Kikuchi *et al.*, Phys. Lett. B391 (1997) 261; T. Kikuchi *et al.*, Eur. Phys. J. A3 (1998) 209.
13. T. Motobayashi *et al.*, Phys. Lett. B264 (1991) 259.
14. T. Gomi *et al.*, in preparation.
15. S. Shimoura *et al.*, Phys. Lett. B348 (1995) 29.
16. T. Nakamura *et al.*, Phys. Rev. Lett. 83 (1999) 1112.
17. T. Teranishi *et al.*, Phys. Lett. B407 (1997) 110.
18. S. Takeuchi *et al.*, Phys. Lett. B515 (2001) 255.
19. S. Shimoura *et al.*, Phys. Lett. B560 (2003) 31.
20. R.F. Casten and N.V. Zamfir, Phys. Lett. 70 (1993) 402.
21. N. Fukunishi, T. Otsuka and T. Sebe, Phys. Lett. B296 (1992) 279.
22. S. Nummela *et al.*, Phys. Rev. C63 (2001) 044316.
23. G. Baur, C.A. Bertulani, and H. Rebel, Nucl. Phys. A458 (1986) 188.
24. J.A. Caggiano *et al.*, Phys. Rev. C64 (2001) 025802.